



Article

Influence of pH and Temperature on the Synthesis and Stability of Biologically Synthesized AgNPs

Oksana Velgosova ¹, Lívia Mačák ^{1,*}, Maksym Lisnichuk ^{2,3} and Peter Varga ¹



- Institute of Materials, Faculty of Materials Metallurgy and Recycling, Technical University of Košice, Letná 9/A, 042 00 Košice, Slovakia; oksana.velgosova@tuke.sk (O.V.)
- Faculty of Science, Institute of Physics, Pavol Jozef Šafárik University in Košice, Park Angelinum 9, 040 01 Košice, Slovakia; maksym.lisnichuk@upjs.sk
- Institute of Materials Research of the Slovak Academy of Sciences, Watsonova 47, 040 01 Košice, Slovakia
- * Correspondence: livia.macak@tuke.sk

Abstract

The synthesis of silver nanoparticles (AgNPs) using sustainable and non-toxic methods has become an important research focus due to the limitations of conventional chemical approaches, which often involve hazardous reagents and produce unstable products. In particular, the effects of reaction conditions on the quality and stability of AgNPs obtained via green synthesis remain insufficiently understood. This study addresses this gap by examining the influence of pH and temperature on the synthesis of AgNPs using Rosmarinus officinalis extract as both reducing and stabilizing agents. UV-vis spectroscopy and TEM analysis revealed that optimal conditions for producing uniform, stable, and spherical AgNPs were achieved at pH 8, with a narrow size distribution (~17.5 nm). At extreme pH values (≤ 3 or ≥ 13), nanoparticle formation was hindered by aggregation or precipitation, while elevated temperatures mainly accelerated reaction without altering particle morphology. HRTEM and SAED confirmed the crystalline face-centered cubic structure, and colloids synthesized at pH 8 showed excellent stability over 30 days. Overall, the results demonstrate that precise pH control is critical for obtaining high-quality AgNPs via a simple, scalable, and environmentally friendly approach. Their stability and homogeneous size highlight potential applications in biomedicine, food packaging, and sensing, where reproducibility and long-term functionality are essential.

Keywords: silver; nanoparticles; green synthesis; pH; temperature; synthesis conditions



Academic Editor: Angelo Maria Taglietti

Received: 12 September 2025 Revised: 25 September 2025 Accepted: 5 October 2025 Published: 10 October 2025

Citation: Velgosova, O.; Mačák, L.; Lisnichuk, M.; Varga, P. Influence of pH and Temperature on the Synthesis and Stability of Biologically Synthesized AgNPs. *Appl. Nano* **2025**, *6*, 22. https://doi.org/10.3390/ applnano6040022

Copyright: © 2025 by the authors. Licensee MDPI, Basel, Switzerland. This article is an open access article distributed under the terms and conditions of the Creative Commons Attribution (CC BY) license (https://creativecommons.org/licenses/by/4.0/).

1. Introduction

Silver nanoparticles (AgNPs) have garnered significant attention in recent decades due to their unique physicochemical properties and wide range of applications in medicine [1,2], environmental remediation [3], food packaging [4], and electronics [5]. Among their most studied features are their potent antimicrobial activity, surface plasmon resonance (SPR), and high surface area-to-volume ratio, which enable enhanced reactivity and functionality [6,7]. While several physical and chemical methods have been developed for the synthesis of AgNPs, increasing concerns over toxicity, environmental impact, and sustainability have led to growing interest in "green" synthesis approaches using biological systems [8,9].

In recent years, the green synthesis of silver nanoparticles (AgNPs) using biological sources has attracted increasing scientific attention. Several recent studies emphasize not only the environmental and biomedical potential of plant- and biomass-derived AgNPs, but

Appl. Nano 2025, 6, 22 2 of 15

also the urgent need to better understand and optimize the synthesis process itself [10–12]. These reviews and experimental works demonstrate that bio-mediated silver nanomaterials are highly promising for a wide range of applications, including photocatalysis, water purification, and antimicrobial treatments. The continued growth of this field confirms its relevance and highlights the importance of exploring key synthesis parameters, such as pH, temperature, and extract composition, that critically affect nanoparticle properties and performance.

Biogenic synthesis of AgNPs involves the use of plant extracts, microorganisms, or biomolecules that act simultaneously as reducing and stabilizing agents. These biosynthetic routes offer several advantages: they are environmentally friendly, cost-effective, energy-efficient, and typically carried out under mild reaction conditions. Among these, plant-mediated synthesis is especially attractive due to its simplicity, scalability, and the complex mixture of phytochemicals (for example, phenolics, flavonoids, alkaloids) that facilitate nanoparticle formation and stabilization.

We selected *Rosmarinus officinalis* leaf extract because it is rich in phenolic compounds, flavonoids, and antioxidant diterpenes (for example, carnosic acid, carnosol), which are known to act as effective electron donors and stabilizing agents in nanoparticle synthesis [13,14]. The high reducing potential of rosemary extract has been demonstrated in previous works, where it successfully mediated the production of silver nanoparticles by reducing Ag^+ ions to Ag^0 [15]. In addition, the antioxidant capacity of rosemary helps to suppress unwanted oxidation or aggregation during synthesis, enhancing nanoparticle stability.

Despite its advantages, green synthesis is highly sensitive to various physicochemical parameters that influence the kinetics of nanoparticle formation, the morphology of the final product, and its long-term stability. Two of the most critical parameters are pH of the precursor solution and temperature at which the synthesis occurs [16]. pH affects the ionization state and reactivity of bioactive compounds in the extract, the reduction potential of silver ions (Ag^+) , and the surface charge of the forming nanoparticles. Similarly, temperature influences the rate of reduction reactions, nucleation dynamics, and the interaction of capping agents with nanoparticle surfaces.

Numerous studies have shown that even small changes in pH and temperature can significantly influence the size, shape, and dispersity of silver nanoparticles (AgNPs), thereby affecting their optical, catalytic, and antimicrobial properties [17,18]. These synthesis conditions also play a crucial role in determining long-term colloidal stability of AgNPs, which is essential for their practical use and storage. For example, nanoparticles formed under suboptimal pH may suffer from aggregation or degradation of the organic stabilizing layer, while excessive thermal input can lead to the denaturation of sensitive biomolecules [11], ultimately reducing both the efficiency of the reduction process and the structural integrity of the nanoparticles.

Although the green synthesis of AgNPs has already been widely explored, the topic remains highly relevant. Continuous optimization of synthesis conditions is necessary to better understand the relationship between parameters and the resulting nanoparticle properties. In this context, our study provides new insights by systematically examining the effect of pH on AgNP synthesis under two different temperature regimes, ambient and elevated (75 °C), within a directly comparable experimental framework. Furthermore, we investigated long-term colloidal stability of the nanoparticles over 30 days, an aspect often overlooked in related research despite its practical importance. By employing an environmentally friendly and easily accessible plant extract, our results help clarify how the interplay between pH and temperature governs nanoparticle formation and stability, thereby contributing meaningful data to the field of green nanotechnology.

Appl. Nano 2025, 6, 22 3 of 15

This study aims to systematically investigate the influence of precursor pH and synthesis temperature on the formation, optical properties, and stability of silver nanoparticles synthesized using a plant-based extract. By combining visual observation, UV-vis spectroscopy, and long-term colloidal monitoring, we seek to determine the optimal conditions for producing stable AgNPs with desirable characteristics. This work contributes to the broader effort to optimize green nanotechnological processes by elucidating the fundamental roles of pH and temperature in nanoparticle biosynthesis.

2. Materials and Methods

2.1. Materials

As silver precursor, silver nitrate (>98% purity) supplied by Mikrochem Ltd. (Pezinok, Slovakia) was employed. The plant material, fresh leaves of *Rosmarinus officinalis* (rosemary) was harvested in summer months from the Botanical Garden in Košice, Slovakia. Nitric acid (HNO₃, 68%, CAS 7697-37-2) and sodium hydroxide (NaOH, pellets, p.a., CAS 1310-73-2), purchased from Fisher Slovakia. To prepare a 20% HNO₃ solution for pH adjustment, 14.28 mL of concentrated nitric acid was diluted with deionized H₂O to a final volume of 100 mL. Similarly, 20 g of NaOH pellets were dissolved in deionized H₂O and diluted to a final volume of 100 mL, yielding a 20% solution that was subsequently used to increase pH. All solutions used in the experiments were prepared using deionized H₂O.

2.2. The Extract Preparation Procedure

Dried rosemary leaves were used for the extract preparation. The preparation procedure was as follows: fresh rosemary leaves (10 g) were dried at 50 °C for 48 h, yielding 2.8 g of dry material, and dry rosemary leaves were mixed with 200 mL of deionized H_2O . This ratio was experimentally optimized and consistently used to ensure comparability, with ~150 mL extract obtained after processing. Subsequently, the mixture was heated to a temperature of 70–80 °C and held at this temperature for 10 min under constant stirring at 800 rpm. After heating, the extract was cooled and filtered. Prepared extract (pH = 5.89) was stored in refrigerator (no longer than 5 days) and used to prepare AgNPs. Extracts were stored at 4 °C for a maximum of 5 days, since longer storage led to degradation and potential contamination from filtration and centrifugation steps.

2.3. AgNP Colloid Preparation Procedure

Two synthesis protocols were employed to evaluate the impact of temperature and pH on the synthesis of AgNPs.

In the first protocol, a precursor solution of Ag^+ ions (400 mL) with a concentration of $c_{Ag} = 50$ mg/L (pH 5.78) was prepared. The silver concentration of 50 mg L⁻¹ was selected based on our previous experiments, as higher concentrations produced excessive amounts of AgNPs, complicating characterization (for example, dilution required for UV-vis, reduced clarity in TEM images). This solution was divided into eight 50 mL Erlenmeyer flasks. The pH in each flask was adjusted to values of 3, 4, 5.5 (natural pH of precursor), 6, 8, 10, 12, and 13. To decrease the pH, a 20% HNO₃ solution was used; to increase the pH, a 20% NaOH solution was applied. After pH adjustment, all precursor solutions were heated in a water bath at 70–80 °C under constant stirring (400 rpm). Once the target temperature was reached, the plant extract was added, and the mixtures were stirred at approximately 70 °C for an additional 20 min. The precursor-to-extract volume ratio was 10:2. The precursor-to-extract volume ratio of 10:2 was selected based on our previous preliminary experiments, in which different ratios were tested to evaluate their influence on nanoparticle formation, stability, and reproducibility.

Appl. Nano 2025, 6, 22 4 of 15

In the second synthesis protocol, the same procedure was followed, except that no heating was applied; all experiments were conducted at ambient temperature.

After synthesis, the UV-vis spectrophotometry was used to confirm AgNP formation. These measurements were labeled as D0. The same measurements were repeated on days 1 (D1), 7 (D7), 14 (D14), and 30 (D30) after synthesis. Selected samples were chosen for TEM and XRD analysis. During the 30-day stability study, colloidal suspensions were stored at room temperature under daylight conditions to simulate simple and practical storage environments. All experiments were repeated three times.

2.4. Methods

The presence and stability of AgNPs were monitored using a UV-vis spectrophotometer (UNICAM UV4, Waltham, MA, USA) in the wavelength range of 300-850 nm. Measurements were performed in 1 cm quartz cuvettes at room temperature (RT). The surface plasmon resonance (SPR) peak position (λ_{max}), peak intensity, and spectral symmetry/broadening were analyzed to assess nanoparticle formation, size distribution, and aggregation behavior. Transmission electron microscopy (TEM, JEOL model JEM-2000FX, Tokyo, Japan), operated at 200 kV, was applied to examine particle size and morphology. Crystallinity was evaluated through selected area electron diffraction (SAED), performed with a JEOL JEM-2100 microscope. Copper grids with deposited samples were used for SAED analysis. High-resolution transmission electron microscopy (HRTEM) was also performed using a JEOL JEM-2100 microscope at 200 kV to resolve lattice fringes and determine interplanar spacings. The chemical composition of nanoparticles was determined by energy-dispersive X-ray spectroscopy (EDX). ImageJ software (version 1.54g) was employed for particle size distribution analysis, evaluating between 300 and 800 nanoparticles. X-ray diffraction (XRD) was used to study phase composition and structure (Malvern Panalytical, Almelo, The Netherlands). The analyses were performed on a Philips X'Pert Pro diffractometer using Cu K α radiation ($\lambda 1 = 1.54056$ Å, $\lambda 2 = 1.54439$ Å) in Bragg–Brentano geometry. Data were collected within a 2θ range of $20-100^{\circ}$ with an RTMS X'Celerator rapid detector.

3. Results and Discussion

3.1. UV-Vis Analysis

Upon mixing the silver precursor solution with the biological extract, an immediate and visible color change was observed in all samples except those with pH 3 and 13. Initially colorless solutions turned yellow to brown, as shown in Figure 1. It was observed that colloidal solutions synthesized at higher temperatures exhibited a slightly darker coloration. This suggests an increased nanoparticle concentration, which is consistent with more efficient reduction and nucleation processes under these conditions. At pH 3 and 13, a precipitate formed rapidly and settled at bottom of the Erlenmeyer flasks, suggesting the formation of large particles that aggregated and subsequently sedimented.

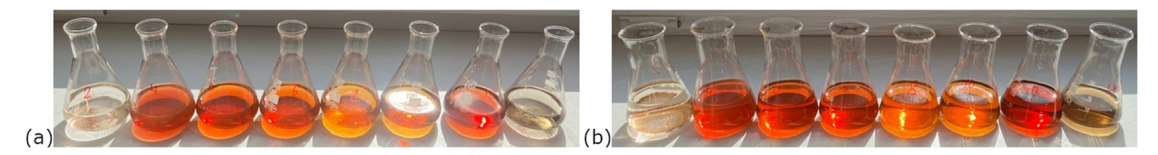


Figure 1. The color of the solutions prepared at 20 $^{\circ}$ C (**a**) and at 75 $^{\circ}$ C (**b**) (from left to right pH 3, 4, 5.5, 6, 8, 10, 12, 13).

The color change observed during synthesis is a primary indicator of silver nanoparticle formation, arising from localized surface plasmon resonance (LSPR). LSPR results from the collective oscillation of conduction electrons in response to incident light and is

Appl. Nano **2025**, 6, 22 5 of 15

sensitive to nanoparticle size, shape, concentration, distribution, and the composition of the surrounding medium. Since visual observation provides only qualitative information, UV-vis absorption spectroscopy (350–850 nm range, quartz cuvette with 1 cm path length, measured at room temperature ~25 °C) is employed to confirm nanoparticle formation through the detection of characteristic LSPR absorption bands. It is well-established that spherical silver nanoparticles exhibit a characteristic LSPR band with maximum absorption peak (ABS_{max}) around 400–450 nm [19–21].

Based on the UV-vis spectra of prepared AgNP colloids (D0—day of synthesis) recorded at different pH values and synthesis temperatures, Figure 2, it can be concluded that pH values ≤ 3 and ≥ 13 are unsuitable for the synthesis of silver nanoparticles. Spectra obtained at pH lower than 5.5 were broader, and ABS_{max} appears at ~450 nm, less symmetric, and exhibited lower absorbance intensity compared to those recorded at pH 6, 8, or 10. The most optimal results in terms of spectral symmetry and intensity were achieved at pH 8 and 10. In these samples, the surface plasmon resonance peaks remained centered around 415 nm, which is characteristic of predominantly spherical AgNPs. This observation aligns with previous studies reporting narrow LSPR bands in 400–440 nm range for spherical nanoparticles of similar size [22–24]. Notably, at pH 12, a secondary shoulder appeared near 540 nm, suggesting either the presence of quasi-spherical particles alongside spherical ones or the formation of two distinct size populations. This broadening and appearance of secondary shoulders can be mechanistically linked to simultaneous nucleation and growth processes occurring under these conditions, where slower kinetics at lower pH favor larger particle growth and aggregation, while faster kinetics at elevated temperatures enhance nucleation efficiency.

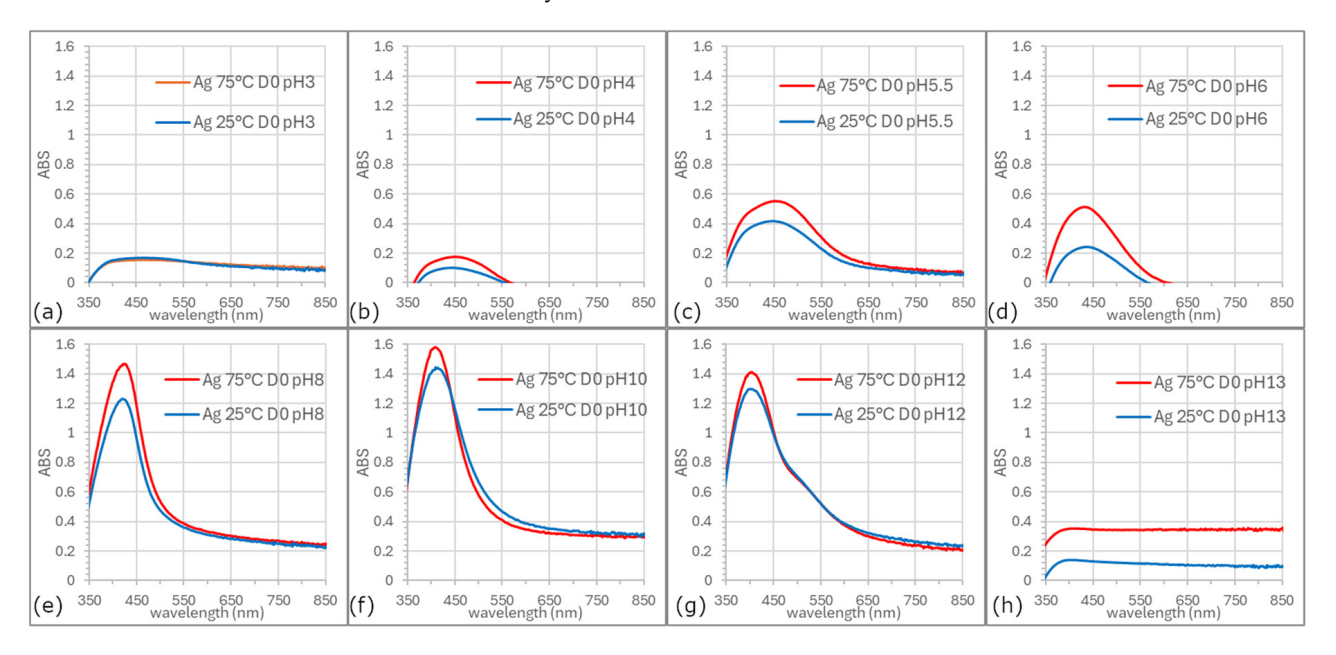


Figure 2. UV-vis spectra of AgNPs synthesized at different pH values on the day of synthesis (D0), measured at 25 $^{\circ}$ C (blue) and 75 $^{\circ}$ C (red). Panels: (a) pH 3, (b) pH 4, (c) pH 5.5, (d) pH 6, (e) pH 8, (f) pH 10, (g) pH 12, (h) pH 13.

From our data and current understanding, we hypothesize that at alkaline pH, the reduction potential of silver ions increases, and the functional groups in the plant extract (such as phenolics, flavonoids, or hydroxyl groups [25–32]) become more ionized and reactive, enhancing their ability to reduce Ag⁺ ions and stabilize the resulting nanoparticles. Conversely, at low pH, these groups may be protonated and less reactive, their functionality apparently increasing even at very high pH (for example, pH 13).

A key finding of this analysis is that the surface plasmon resonance profiles remained consistent at the same pH values, regardless of whether the synthesis was performed at ambient or elevated temperatures. This suggests that the morphology of the nanoparticles was not significantly influenced by temperature. However, synthesis temperature had a clear impact on efficiency of AgNP formation, the reaction rate, and to a minor extent the nanoparticle size.

Higher temperatures led to increased synthesis efficiency, likely due to enhanced reaction kinetics. Alahmad et al. [33] also reported that AgNPs were formed more rapidly at elevated temperatures. Similarly, Kaabipour et al. [34] observed that lowering the synthesis temperature resulted in a broader SPR peak, which they attributed to a wider size distribution, though the morphology of the nanoparticles remained unchanged.

3.2. Concentration of AgNPs in Colloid

UV-vis spectral analysis provides insights not only into the presence of nanoparticles, their size, shape, and stability over time but also into their concentration. Sikder et al. in their work demonstrated that UV-vis spectroscopy, owing to the unique size-dependent properties of nanoparticles, can be used as a detection method to measure the concentration of AgNPs [35]. The ABS_{max} intensity can reflect the synthesis yield. Higher intensities generally indicate a higher nanoparticle concentration. By applying the Lambert-Beer law it is possible to approximate the concentration of nanoparticles in the colloidal solution. Based on calculations, the highest yields of silver nanoparticles were recorded at pH 8 and 10, regardless of the process temperature. However, when comparing these calculated values with the initial concentration of the AgNO₃ precursor (50 mg/L), it was found that the theoretically determined concentrations of AgNPs were significantly lower (0.129 mg/L, the ϵ_{λ} = 2.16 × 10¹¹ L/mol·cm). This discrepancy between absorbance, the applied calculation, and the known concentration of Ag⁺ ions in the reaction mixture (assuming complete reduction of Ag⁺ to metallic silver) is likely due to several factors [36–40].

Most studies that use Lambert–Beer law to calculate AgNP concentration rely on a standardized value of the molar absorption coefficient (for example, $\varepsilon \approx 3 \times 10^{10}\, L/mol\cdot cm$ for 10 nm spherical particles). However, this value was established for highly monodisperse, synthetically produced nanoparticles under strictly defined conditions. In the case of biological or "green" synthesis, where complex organic molecules stabilize particles, the effective ε value may be significantly lower. For example, according to literature [36], ε for spherical nanoparticles with a diameter of 20 nm and an ABS_{max} at 400 nm, prepared using citrate, is $0.418 \times 10^{10}\, L/mol\cdot cm$. Due to this uncertainty in the ε value, the calculated concentration may be underestimated when a standard ε is applied. Similarly, low concentration values compared to the inlet concentration were reported in the works of Alahmad et al. [33] and Peiris et al. [41]. Both authors demonstrated that the correct choice of the extinction coefficient is crucial, as it directly depends on the wavelength and particle size. With increasing λ_{max} and larger particle size, the extinction coefficient increases.

Another factor may be light scattering instead of absorption. Silver nanoparticles, especially those with diameters greater than 10 nm, exhibit significant light scattering. The Lambert-Beer law assumes purely absorptive behavior. As a result, the measured absorbance can become nonlinear and may not directly correspond to particle concentration [37]. Scattering also causes broadening and distortion of the plasmonic band, making it difficult to precisely determine the absorbance maximum and potentially leading to an inaccurate calculation of the concentration.

Surface passivation and stabilizers may also affect calculated values. Biologically synthesized AgNPs are often passivated by a layer of biomolecules (for example, phenols, flavonoids, carbohydrates), which bind to the particle surface and prevent agglomeration.

This layer may partially shield the plasmon resonance, thereby lowering the absorbance intensity. Although the nanoparticles may be stable and present at high concentration, optically they appear weaker, which results in an artificially low yield as estimated by UV-vis spectroscopy. For example, Chandra et al. studied the interaction of AgNPs with (–)-epigallocatechin gallate (EGCG) and found that EGCG not only reduces Ag⁺ but also chelates AgNPs, slightly altering their SPR band, causing a shift and suppression of the signal [38]. Malik et al. reported that polyphenols and other biomolecules present in the extract (for example, chlorogenic acid, luteolins, cynaropicrin, polysaccharides, and saponins) bind to the AgNP surface and influence the shape and intensity of the plasmon band [39].

Despite the assumption of complete reduction based on intense color formation, it is not certain that all Ag^+ ions were converted. Residual Ag^+ ions may be bound in complexes with reducing agents or stabilizers or may remain unreacted. As a result, only partial precursor conversion may have occurred, even if the synthesis appears visually successful. Therefore, it must be concluded that the Lambert-Beer law provides only an approximate estimate of AgNP concentration, which can be significantly distorted in a complex matrix and biological synthesis. More accurate quantification of yield would require the use of analytical methods such as Sp-ICP-OES (Single Particle Inductively Coupled Plasma Mass Spectrometry), NTA (Nanoparticle Tracking Analysis) or AAS (Atomic Absorption Spectrometry), or alternatively, yield determination using a calibration curve created specifically for the given particle type and conditions.

The Lambert–Beer calculation likely underestimated the absolute concentration of silver nanoparticles due to the extinction coefficient used. However, based on the colloid color and the UV-vis spectra, it follows that nearly all Ag⁺ ions were converted into AgNPs. Despite this limitation, the systematic deviation would have affected all samples similarly. Therefore, while the absolute yields may appear low, the relative differences between the samples remain reliable and valid for comparative analysis.

3.3. Transmission Electron Microscopy Analysis

Based on the analysis of UV-vis absorption spectra, the synthesized AgNP samples were classified into three groups, Figure 3a, according to the similarity of their optical properties:

- Group I: samples synthesized at pH \leq 6;
- Group II: sample synthesized at pH 8;
- Group III: samples synthesized at pH \geq 10.

To enable detailed morphological characterization, representative samples from each group (pH 5.5, 8, and 12; at both synthesis temperatures) were selected and analyzed using Transmission Electron Microscopy. The pH 10 sample was not included in the long-term stability tests because its UV–vis spectrum was nearly identical to that of the pH 8 sample, indicating very similar nanoparticle characteristics. For practical reasons, pH 8 was selected for the extended stability study, as achieving this pH required a smaller addition of base, minimizing potential alterations to the colloidal system. The analysis focused on particle shape, size, and size distribution. TEM characterization was performed one day after synthesis (D1) to allow sufficient time for nucleation and nanoparticle growth. TEM micrographs of the selected samples are presented in Figure 3.

For comparison purposes, all UV-vis spectra were normalized to their maximum absorbance, $ABS_{max} = 1$, Figure 3a. These normalized spectra enable a more accurate evaluation of peak shapes and wavelength shifts between samples. No significant differences were observed in the UV-vis absorption spectra of the samples synthesized at 75 °C compared to those prepared at ambient temperature, Figure 3a. This was further confirmed

Appl. Nano 2025, 6, 22 8 of 15

by TEM micrographs, Figure 3b–g, and particle size distribution histograms, Figure 3h,i, which showed that neither morphology nor size of the nanoparticles was substantially affected by the synthesis temperature. In contrast, the precursor pH had a pronounced influence on both nanoparticle size and shape.

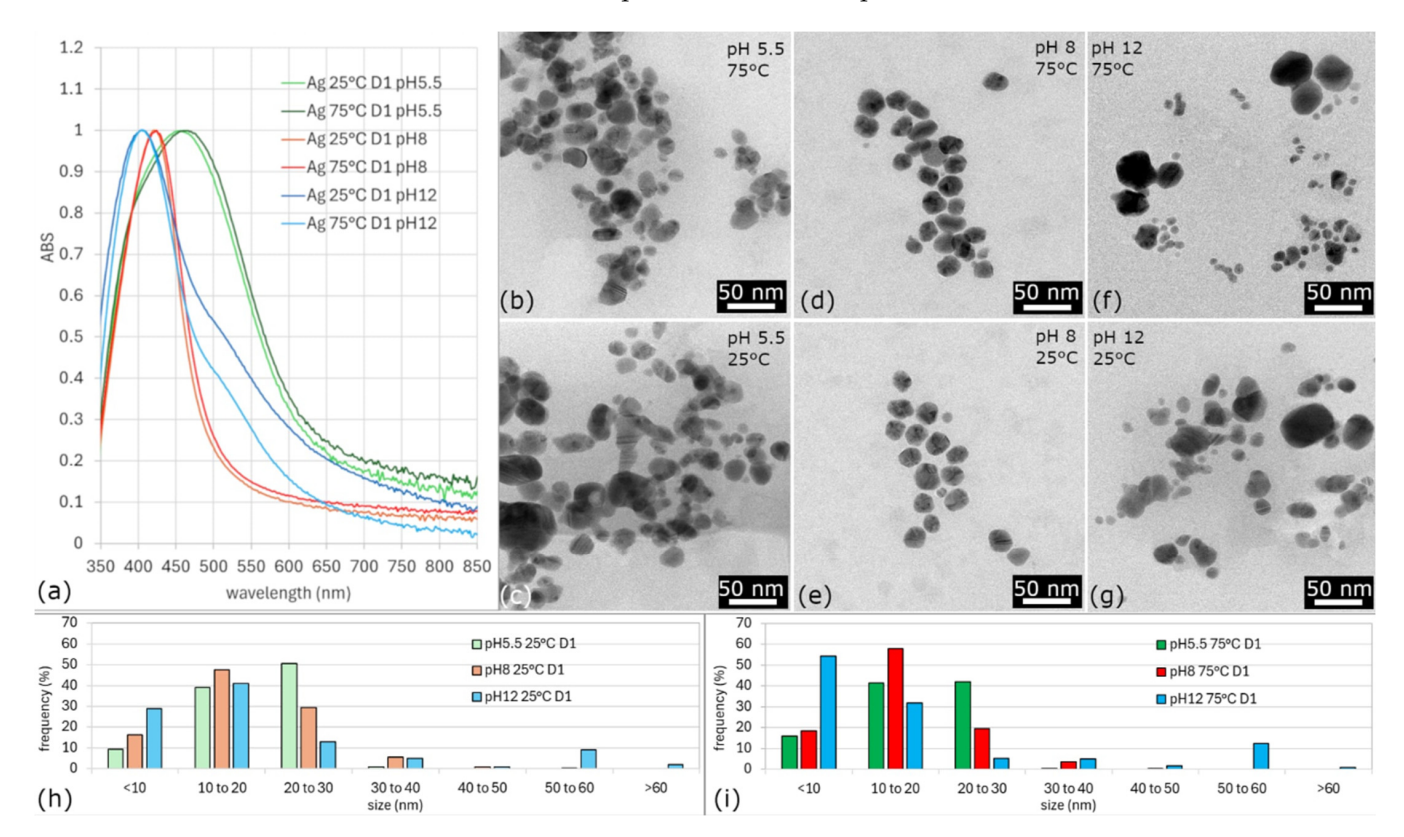


Figure 3. Approximated UV-vis spectra of AgNPs synthesized at pH 5.5, 8, and 12 at 25 $^{\circ}$ C and 75 $^{\circ}$ C on D1 (a). TEM microphotographs of AgNPs at pH 5.5 (b,c), pH 8 (d,e), and pH 12 (f,g) for 75 $^{\circ}$ C and 25 $^{\circ}$ C, respectively. Size distribution histograms for nanoparticles synthesized at temperatures of 25 $^{\circ}$ C (h) and 75 $^{\circ}$ C (i).

At pH 5.5, quasi-spherical nanoparticles were formed in both cases, with average diameters of 17 nm for the thermally assisted synthesis and 18.5 nm for the ambient-temperature synthesis, also larger nanoparticles of more than 30 nm occurred in both samples. The absorption spectra of colloids prepared at pH 5.5 are broader compared to those synthesized at pH 8, Figure 3a, indicating a wider size distribution and less uniform particle shape.

In contrast, nanoparticles synthesized at pH 8 showed a narrower size distribution and mostly spherical shapes, as confirmed by the TEM images, Figure 3d,e, and histograms, Figure 3h,i. For both synthesis temperatures at pH 8, the average particle size was about 17.5 nm.

At pH 12, the UV-vis spectra showed an extra shoulder at higher wavelengths, indicating the presence of larger quasi-spherical particles alongside smaller ones, which was also confirmed by size distribution analysis, Figure 3h,i. TEM analysis, Figure 3f,g, verified that the most symmetrical and monodisperse nanoparticles were produced at pH 8, regardless of the synthesis temperature.

Several studies have investigated the effect of pH on the synthesis and properties of silver nanoparticles (AgNPs). Fernando et al. examined how pH influences the stability, aggregation, and dissolution of pre-formed AgNPs, finding that higher pH reduces aggregation, decreases particle size, and enhances colloidal stability, which indicates that pH

exerts a stronger effect than other environmental factors such as ionic concentration [42]. Similarly, Miranda et al. studied the green synthesis of AgNPs using Spinacia oleracea leaf extract at pH values of 4, 5, and 9. Their results showed that nanoparticles synthesized under more alkaline conditions were more stable and moreover, exhibited stronger and longer-lasting antimicrobial activity [43]. Norouzi et al. explored the chemical reduction synthesis of AgNPs over a wide pH range (2–13), reporting that pH 10 produced the smallest (3–6 nm), most monodisperse, and most stable particles, while pH 13 led to the precipitation of silver compounds [44]. In agreement with these findings, our study demonstrated that alkaline pH, at our conditions, pH 8, is optimal for forming uniform, stable, and monodisperse spherical AgNPs, with an average diameter of approximately 18 nm and high structural integrity. Moreover, the long-term colloidal stability of AgNPs was found to be strongly pH-dependent, with slightly alkaline conditions offering the most favorable electrostatic stabilization over time.

In our study, a clear correlation was observed between the color of the colloidal solutions, nanoparticle morphology, and particle concentration. Since all prepared AgNPs were predominantly spherical or quasi-spherical in shape, as confirmed by TEM analysis, the color of the colloids remained within the same honey-brown range, which is characteristic of spherical silver nanoparticles due to their uniform LSPR response. The variations among samples were mainly reflected in the color intensity (saturation) rather than in hue. This difference is directly related to nanoparticle concentration, as supported by UV-vis spectra: samples with higher absorbance maxima (ABSmax) exhibited more intense coloration, indicating a higher number of nanoparticles in the solution. Thus, the observed relationship between color, concentration, and morphology can be attributed to the influence of nanoparticle number and size distribution on LSPR behavior, with concentration being the key factor responsible for the changes in visual appearance.

3.4. EDS, HRTEM and EDX Analysis of Nanoparticles

The EDS characterization confirmed the presence of silver in all analyzed samples. Figure 4a presents a representative spectrum of nanoparticles synthesized at pH 8 and 75 °C. A strong silver signal is presented, but other elements such as Cu and Na are also obvious. The Cu signal is caused by the copper grid, which was used in sample preparation, and Na is a residue from the pH treatment. The presence of Cu as an artifact was well-documented and described by Jianqiang Hu et al. [45], who reported that copper grids can produce spurious Cu signals due to electron scattering.

The HRTEM image of the sample synthesized at pH 8, Figure 4b, shows lattice fringes with spacings of 0.2795, 0.2447, and 0.301 nm (measured over 14 atoms), which confirms the crystalline nature of the synthesized AgNPs. These interplanar distances likely correspond to different crystallographic directions of the face-centered cubic (FCC) structure of silver, although the exact indices (hkl) are not identified. Additionally, the corresponding selected area electron diffraction (SAED) pattern, Figure 4c, displays well-defined diffraction rings indexed to the (111), (200), (220), and (311) planes, further confirming the FCC crystalline structure of AgNPs.

X-ray diffraction (XRD) analysis was performed to determine the crystallographic phases present in the samples by comparing the obtained diffraction patterns with the PDF-2 database (Powder Diffraction File). The diffraction peaks observed at 2θ values of 38.10° , 44.37° , 64.18° , and 77.55° , Figure 5, correspond to the (111), (200), (220), and (311) planes, respectively, which are characteristic of crystalline silver (PDF 00-001-1167). Quantitative phase analysis indicated that silver accounted for 91.6% of the sample composition. In addition, diffraction peaks corresponding to silver chloride (AgCl, PDF 00-031-1238) were detected, Table 1.

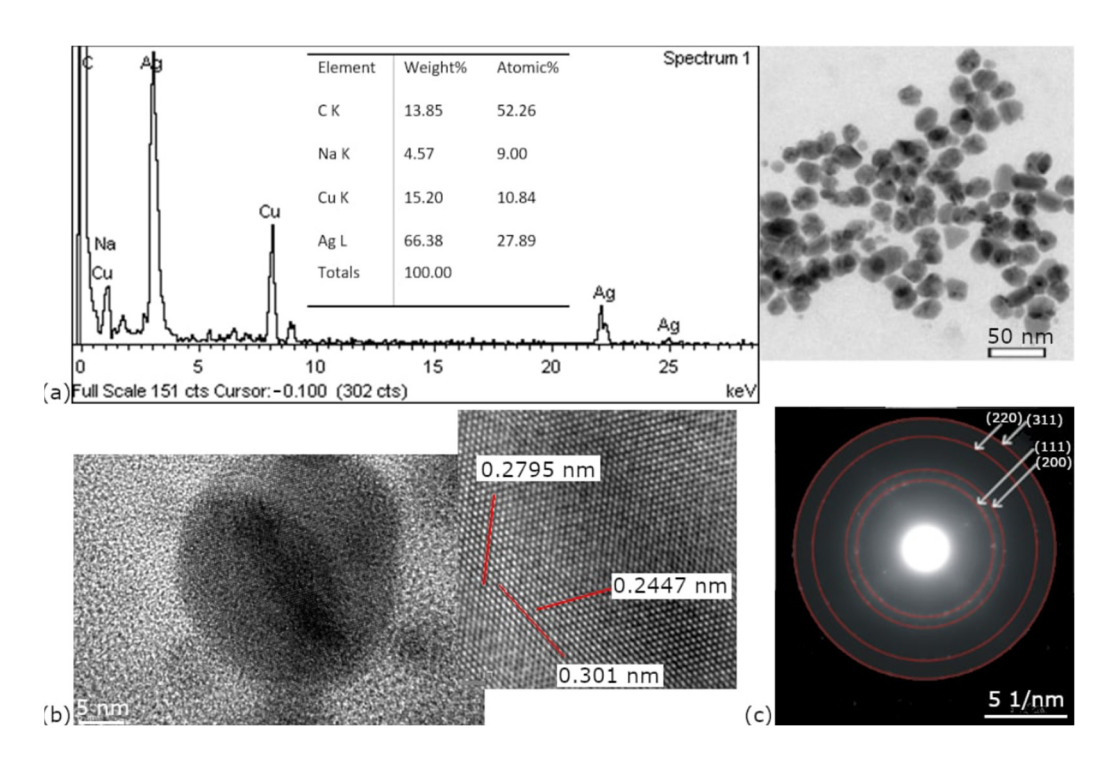


Figure 4. EDS analysis (**a**), HRTEM image, and lattice fringes (**b**), and electron diffraction (**c**) of the AgNPs prepared at a temperature of 75 °C at pH 8.

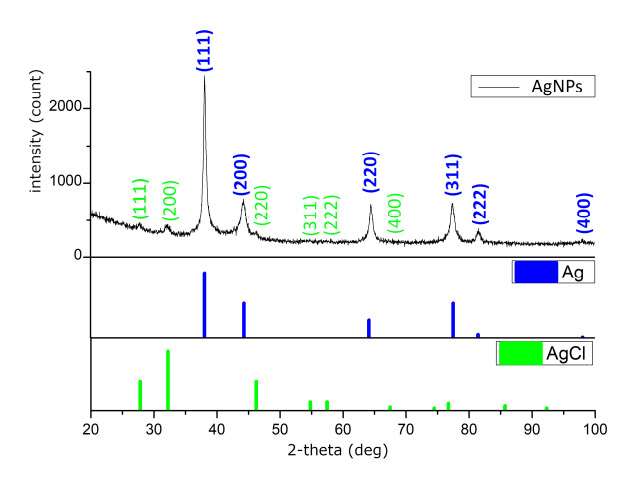


Figure 5. XRD analysis of the AgNPs prepared at a temperature of 75 $^{\circ}$ C at pH 8.

Table 1. Analysis of AgNPs prepared at a temperature of 75 °C at pH 8.

Sample	Lattice	Space Group	vol. Percentage (%)
Ag	cubic	Fm-3m	91.6
AgCl	cubic	Fm-3m	8.4

The identification of these reflections confirms that the silver nanoparticles adopt a cubic crystal structure, specifically a face-centered cubic (FCC) lattice, in which the unit cell is a cube with equal edge lengths and 90° interaxial angles. The assigned space group, Fm-3m, denotes the high-symmetry nature of the lattice, including mirror planes and multiple rotational axes, and is consistent with the most stable form of metallic silver.

The presence of AgCl detected in our XRD patterns can be explained by the occurrence of chloride ions (Cl⁻) in the plant extracts used for the synthesis. Chlorides are naturally present in many plants as mineral salts (for example, NaCl, KCl) [46,47] or may originate from the growth medium and water [48] used during extract preparation. During the

reduction of Ag⁺ to Ag⁰, Cl⁻ ions can react with silver ions to form insoluble AgCl, which may precipitate alongside AgNPs. This phenomenon has been reported in several studies on green synthesis of silver nanoparticles using plant extracts, where AgCl was identified as a secondary phase in XRD patterns due to the presence of chlorides in the biological medium [46–48]. The formation of AgCl in such systems is therefore considered a common and well-documented outcome rather than contamination.

3.5. Stability of AgNPs

Figures 6 and 7 illustrate evolution of SPR bands in colloids synthesized at ambient temperature and 75 °C across various pH values over 30 days. Colloids prepared at elevated temperatures generally exhibited higher stability.

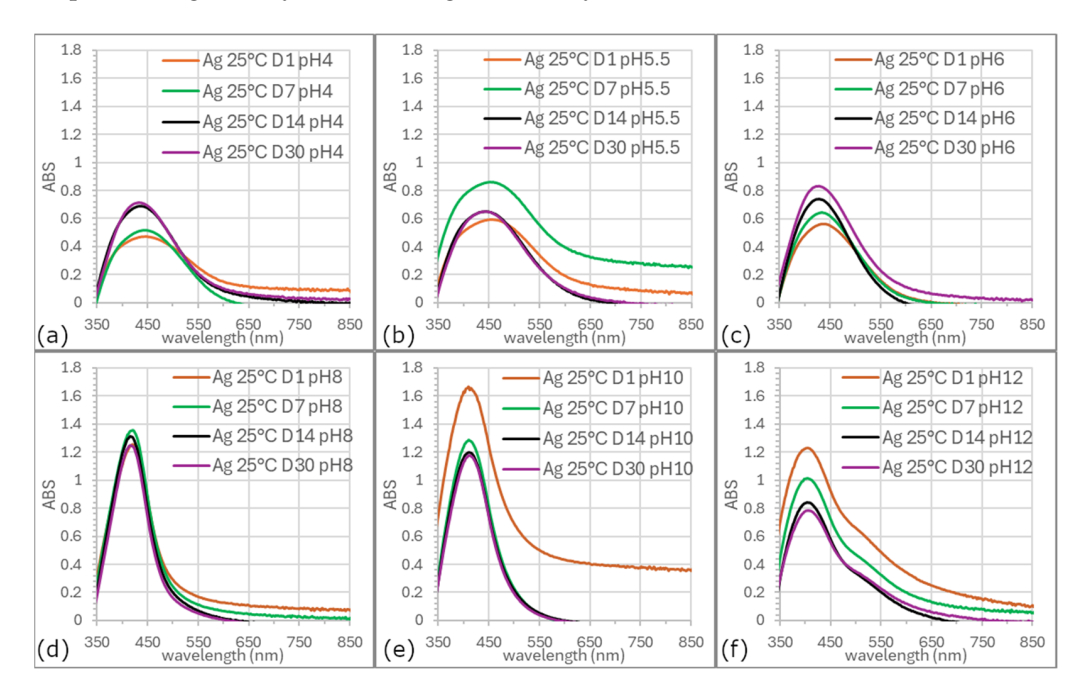


Figure 6. UV-vis spectra showing the evolution of SPR bands of AgNP colloids synthesized at 25 °C over time (D1, D7, D14, D30) at different pH values: (a) pH 4, (b) pH 5.5, (c) pH 6, (d) pH 8, (e) pH 10, and (f) pH 12.

Long-term stability was maintained at pH 6, 8, and 12, although SPR spectrum at pH 6 was broader and the band symmetry at pH 12 was the lowest. The most favorable properties as excellent stability, uniform morphology, controlled size distribution, and the highest yield were consistently obtained for AgNPs synthesized at a precursor pH of 8.

The pH plays a decisive role in the long-term stability of biologically synthesized silver nanoparticles. Stability is strongly influenced by surface charge, which governs electrostatic repulsion and prevents aggregation. Literature reports indicate that AgNPs reach maximum stability under slightly alkaline conditions, where optimized zeta potential minimizes clustering [41,49]. In contrast, strongly acidic or highly alkaline conditions reduce stability, either by weakening electrostatic repulsion or by degrading organic capping molecules from the plant extract [50]. Our 30-day observations are in agreement with these findings. Moreover, several studies note that extreme pH can promote AgNP oxidation or dissolution, compromising morphological integrity and plasmonic properties. Therefore, maintaining an appropriate pH during both storage and application is essential to preserve the physical and chemical stability of AgNPs.

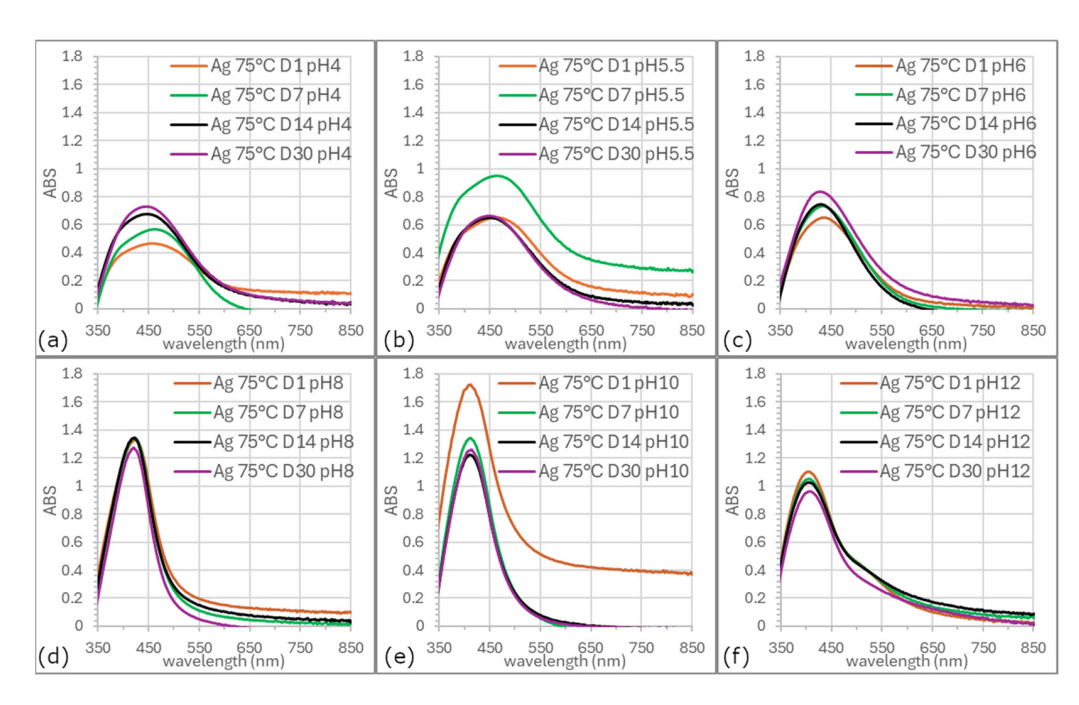


Figure 7. UV-vis spectra showing the evolution of SPR bands of AgNP colloids synthesized at 75 °C over time (D1, D7, D14, D30) at different pH values: (a) pH 4, (b) pH 5.5, (c) pH 6, (d) pH 8, (e) pH 10, and (f) pH 12.

4. Conclusions

Biological (green) synthesis represents a promising method for the preparation of silver nanoparticles with low environmental impact. This work demonstrates successful green synthesis of silver nanoparticles using Rosmarinus officinalis extract under varying pH and temperature conditions. UV-vis spectroscopy and TEM imaging revealed that pH 8 provides optimal conditions for the formation of uniform, stable, and monodisperse spherical nanoparticles with an average diameter of ~17.5 nm, high yield, and excellent colloidal stability for at least 30 days. Their high structural integrity was confirmed by HRTEM and SAED, while XRD analysis verified crystalline FCC structure. Notably, the synthesis temperature did not significantly affect nanoparticle morphology, although elevated temperatures enhanced the reaction rate and efficiency, which facilitates transfer of process to production. The long-term colloidal stability of AgNPs was shown to depend strongly on pH, with slightly alkaline conditions providing the most favorable electrostatic stabilization. Although biological synthesis is often limited by the complex and variable composition of plant extracts, our findings provide a practical guideline for standardization, enabling this green approach to become applicable on an industrial scale. Future studies will incorporate advanced quantification techniques such as Sp-ICP-OES, NTA, or AAS to achieve a more precise characterization of AgNPs.

This paves the way for industrial production of stable AgNPs and their commercialization (for example, for antibacterial materials, food packaging, or sensing applications), where colloids prepared by chemical synthesis still dominate due to synthetic reagents and established large-scale production.

Author Contributions: Conceptualization, O.V.; methodology, L.M., M.L., and O.V.; validation, P.V., L.M.; formal analysis, L.M., M.L., and P.V.; investigation, O.V., L.M., M.L., and P.V.; data curation, M.L.; writing—original draft preparation, O.V.; writing—review and editing, O.V. and L.M.; visualization, P.V.; supervision, O.V. All authors have read and agreed to the published version of the manuscript.

Funding: This research received no external funding.

Data Availability Statement: All data are available from the corresponding author upon reasonable request.

Acknowledgments: KEGA 011TUKE-4/2025 Modern Materials for Energy: Innovative Education for Enhancing the Quality of Teaching Materials Engineering Subjects.

Conflicts of Interest: The authors declare no conflicts of interest.

References

- 1. Melo, R.M.; Albuquerque, G.M.; Monte, J.P.; Pereira, G.A.L.; Pereira, G. Recent Advances in the Application of Silver Nanoparticles for Enhancing Phototherapy Outcomes. *Pharmaceuticals* **2025**, *18*, 970. [CrossRef]
- 2. Meher, A.; Tandi, A.; Moharana, S.; Chakroborty, S.; Mohapatra, S.S.; Mondal, A.; Dey, S.; Chandra, S. Silver nanoparticle for biomedical applications: A review. *Hybrid Adv.* **2024**, *6*, 100184. [CrossRef]
- Silva-Holguín, P.N.; Garibay-Alvarado, J.A.; Reyes-López, S.Y. Silver Nanoparticles: Multifunctional Tool in Environmental Water Remediation. *Materials* 2024, 17, 1939. [CrossRef]
- Kraśniewska, K.; Galus, S.; Gniewosz, M. Biopolymers-Based Materials Containing Silver Nanoparticles as Active Packaging for Food Applications—A Review. *Int. J. Mol. Sci.* 2020, 21, 698. [CrossRef] [PubMed]
- 5. Zhao, W.; Natsuki, J.; Trung, V.D.; Li, H.; Tan, J.; Yang, W.; Natsuki, T. AgNPs/CNTs modified nonwoven fabric for PET-based flexible interdigitated electrodes in pressure sensor applications. *Chem. Eng. J.* **2024**, *499*, 156252. [CrossRef]
- 6. Huq, M.A.; Ashrafudoulla, M.; Rahman, M.M.; Balusamy, S.R.; Akter, S. Green Synthesis and Potential Antibacterial Applications of Bioactive Silver Nanoparticles: A Review. *Polymers* **2022**, *14*, 742. [CrossRef]
- 7. Bruna, T.; Maldonado-Bravo, F.; Jara, P.; Caro, N. Silver Nanoparticles and Their Antibacterial Applications. *Int. J. Mol. Sci.* **2021**, 22, 7202. [CrossRef]
- 8. Fahim, M.; Shahzaib, A.; Nishat, N.; Jahan, A.; Bhat, T.A.; Inam, A. Green Synthesis of Silver Nanoparticles: A Comprehensive Review of Methods, Influencing Factors, and Applications. *JCIS Open* **2024**, *16*, 100125. [CrossRef]
- 9. Bedlovičová, Z.; Siksa, P.; Kováčová, M.; Bureš, R.; Tkáčiková, L.; Džunda, R.; Tampubolon, I.O.; Balážová, L.; Baláž, M. Lavender-Mediated Solvent-Free Biomechanochemical Synthesis of Antibacterially Active Ag/AgCl Nanoparticles Using a Taguchi Design. Adv. Nat. Sci. Nanosci. Nanotechnol. 2025, 16, 015018. [CrossRef]
- 10. Sehar, S.; Sehrish, F.; Qurat, U.A.; Zunaira, S.; Janjua, M.R.S.A. A review on green synthesis of silver nanoparticles (SNPs) using plant extracts: A multifaceted approach in photocatalysis, environmental remediation, and biomedicine. *RSC Adv.* **2025**, *15*, 3858–3903. [CrossRef]
- 11. Kumar, D.; Kumar, S.; Gholap, A.D.; Kumari, R.; Tanwar, R.; Kumar, V.; Faiyazuddin, M. A comprehensive review on the biomass-mediated synthesis of silver nanoparticles: Opportunities and challenges. *J. Environ. Chem. Eng.* **2025**, *3*, 115133. [CrossRef]
- 12. Sidorowicz, A.; Atzori, F.; Zedda, F.; Fais, G.; Loy, F.; Licheri, R.; Lai, N.; Desogus, F.; Cao, G.; Concas, A. Novel experimental and theoretical study on the synthesis and use of microalgae-derived silver nanomaterials for water purification. *J. Water Process Eng.* **2025**, *69*, 106831. [CrossRef]
- 13. Andrade, J.M.; Faustino, C.; Garcia, C.; Ladeiras, D.; Reis, C.P.; Rijo, P. Rosmarinus officinalis L.: An update review of its phytochemistry and biological activity. Future Sci. OA 2018, 4, FSO283. [CrossRef] [PubMed]
- 14. Ghaedi, M.; Yousefinejad, M.; Safarpoor, M.; Zare Khafri, H.; Purkait, M.K. *Rosmarinus officinalis* leaf extract mediated green synthesis of silver nanoparticles and investigation of its antimicrobial properties. *J. Ind. Eng. Chem.* 2015, 31, 167–172. [CrossRef]
- 15. Dhouibi, N.; Manuguerra, S.; Arena, R.; Messina, C.M.; Santulli, A.; Kacem, S.; Dhaouadi, H.; Mahdhi, A. Impact of the Extraction Method on the Chemical Composition and Antioxidant Potency of *Rosmarinus officinalis* L. Extracts. *Metabolites* **2023**, *13*, 290. [CrossRef]
- 16. Ariski, R.T.; Lee, K.K.; Kim, Y.; Lee, C.-S. The impact of pH and temperature on the green gold nanoparticles preparation using Jeju Hallabong peel extract for biomedical applications. *RSC Adv.* **2024**, *14*, 14582–14592. [CrossRef]
- 17. Srikar, S.K.; Giri, D.D.; Pal, D.B.; Mishra, P.K.; Upadhyay, S.N. Green Synthesis of Silver Nanoparticles: A Review. *Green Sustain. Chem.* **2016**, *6*, 34–56. [CrossRef]
- 18. Wirwis, A.; Sadowski, Z. Green Synthesis of Silver Nanoparticles: Optimizing Green Tea Leaf Extraction for Enhanced Physicochemical Properties. *ACS Omega* **2023**, *8*, 30532–30549. [CrossRef]
- 19. Annamalai, J.; Nallamuthu, T. Green synthesis of silver nanoparticles: Characterization and determination of antibacterial potency. *Appl. Nanosci.* **2016**, *6*, 259–265. [CrossRef]
- 20. Zhang, X.F.; Liu, Z.G.; Shen, W.; Gurunathan, S. Silver Nanoparticles: Synthesis, Characterization, Properties, Applications, and Therapeutic Approaches. *Int. J. Mol. Sci.* **2016**, *17*, E1534. [CrossRef] [PubMed]

Appl. Nano 2025, 6, 22 14 of 15

21. Subhan, A.; Dharmalingam, K.; Mourad, A.H.I.; Mahmoud, S.T.; Alawadhi, H. Improved photovoltaic performance of dye-sensitized solar cell upon doping with pulsed-laser fabricated plasmonic silver nanoparticles as modified photoanodes. *Mater. Renew. Sustain. Energy* 2025, 14, 39. [CrossRef]

- 22. Patil, R.B.; Chougale, A.D. On the shape based SPR of silver nanostructures. Int. J. Nanotechnol. 2021, 18, 1015–1027. [CrossRef]
- 23. Kotakadi, V.S.; Gaddam, S.A.; Venkata, S.K.; Sarma, P.V.; Sai Gopal, D.V. Biofabrication and spectral characterization of silver nanoparticles and their cytotoxic studies on human CD34+ve stem cells. *3 Biotech* **2016**, *6*, 216. [CrossRef]
- 24. Raza, M.A.; Kanwal, Z.; Rauf, A.; Sabri, A.N.; Riaz, S.; Naseem, S. Size- and Shape-Dependent Antibacterial Studies of Silver Nanoparticles Synthesized by Wet Chemical Routes. *Nanomaterials* **2016**, *6*, 74. [CrossRef] [PubMed]
- 25. Iravani, S. Green Synthesis of Metal Nanoparticles Using Plants. Green Chem. 2011, 13, 2638–2650. [CrossRef]
- 26. Mittal, A.K.; Chisti, Y.; Banerjee, U.C. Synthesis of Metallic Nanoparticles Using Plant Extracts. *Biotechnol. Adv.* **2013**, *31*, 346–356. [CrossRef]
- 27. Ahmed, S.; Ahmad, M.; Swami, B.L.; Ikram, S. A Review on Plants Extract Mediated Synthesis of Silver Nanoparticles for Antimicrobial Applications: A Green Expertise. *J. Adv. Res.* **2016**, 7, 17–28. [CrossRef] [PubMed]
- 28. Mikhailova, E.O. Green Silver Nanoparticles: An Antibacterial Mechanism. Antibiotics 2025, 14, 5. [CrossRef]
- 29. Khalil, M.M.H.; Ismail, E.H.; El-Baghdady, K.Z.; Mohamed, D. Green Synthesis of Silver Nanoparticles Using Olive Leaf Extract and Its Antibacterial Activity. *Arab. J. Chem.* **2014**, *7*, 1131–1139. [CrossRef]
- 30. Prasad, R.; Pandey, R.; Barman, I. Engineering Tailored Nanoparticles with Microbes: Quo Vadis? *Wiley Interdiscip. Rev. Nanomed. Nanobiotechnol.* **2016**, *8*, 316–330. [CrossRef]
- 31. Bar, H.; Bhui, D.K.; Sahoo, G.P.; Sarkar, P.; Pyne, S.; Misra, A. Green Synthesis of Silver Nanoparticles Using Seed Extract of Jatropha Curcas. *Colloids Surf. A Physicochem. Eng. Asp.* **2009**, *348*, 212–216. [CrossRef]
- 32. Singh, P.; Kim, Y.J.; Zhang, D.; Yang, D.C. Biological Synthesis of Nanoparticles from Plants and Microorganisms. *Trends Biotechnol.* **2016**, *34*, 588–599. [CrossRef]
- 33. Alahmad, A.; Feldhoff, A.; Bigall, N.C.; Rusch, P.; Scheper, T.; Walter, J.-G. Hypericum perforatum L.-Mediated Green Synthesis of Silver Nanoparticles Exhibiting Antioxidant and Anticancer Activities. *Nanomaterials* **2021**, *11*, 487. [CrossRef] [PubMed]
- 34. Sikder, M.; Lead, J.R.; Chandler, G.T.; Baalousha, M. A rapid approach for measuring silver nanoparticle concentration and dissolution in seawater by UV–Vis. *Sci. Total Environ.* **2018**, *618*, 597–607. [CrossRef]
- 35. Kaabipour, S.; Hemmati, S. A review on the green and sustainable synthesis of silver nanoparticles and one-dimensional silver nanostructures. *Beilstein J. Nanotechnol.* **2021**, *12*, 102–136. [CrossRef] [PubMed]
- 36. Paramelle, D.; Sadovoy, A.; Gorelik, S.; Free, P.; Hobley, J.; Fernig, D.G. A Rapid Method to Estimate the Concentration of Citrate Capped Silver Nanoparticles from UV-Visible Light Spectra. *Analyst* **2014**, *139*, 4855–4861. [CrossRef]
- 37. Kelly, K.L.; Coronado, E.; Zhao, L.L.; Schatz, G.C. The Optical Properties of Metal Nanoparticles: The Influence of Size, Shape, and Dielectric Environment. *J. Phys. Chem. B* **2003**, 107, 668–677. [CrossRef]
- 38. Chandra, G.K.; Tripathy, D.R.; Dasgupta, S.; Roy, A. Interaction of (—)-Epigallocatechin Gallate with Silver Nanoparticles. *arXiv* **2010**, arXiv:1001.0285. [CrossRef]
- 39. Malik, M.A.; Batterjee, M.G.; Kamli, M.R.; Alzahrani, K.A.; Danish, E.Y.; Nabi, A. Polyphenol-Capped Biogenic Synthesis of Noble Metallic Silver Nanoparticles for Antifungal Activity against Candida Auris. *J. Fungi* 2022, *8*, 639. [CrossRef]
- 40. Abkhalimov, E.; Ershov, V.; Ershov, B. Determination of the Concentration of Silver Atoms in Hydrosol Nanoparticles. *Nanomate-rials* **2022**, 12, 3091. [CrossRef]
- 41. Peiris, M.K.; Gunasekara, C.P.; Jayaweera, P.M.; Arachchi, N.D.; Fernando, N. Biosynthesized silver nanoparticles: Are they effective antimicrobials? *Mem. Do Inst. Oswaldo Cruz* **2017**, *112*, 537–543. [CrossRef]
- 42. Fernando, I.; Zhou, Y. Impact of pH on the stability, dissolution and aggregation kinetics of silver nanoparticles. *Chemosphere* **2019**, 216, 297–305. [CrossRef] [PubMed]
- 43. Miranda, A.; Akpobolokemi, T.; Chung, E.; Ren, G.; Raimi-Abraham, B.T. pH Alteration in Plant-Mediated Green Synthesis and Its Resultant Impact on Antimicrobial Properties of Silver Nanoparticles (AgNPs). *Antibiotics* **2022**, *11*, 1592. [CrossRef]
- 44. Sartori, P.; Delamare, A.P.L.; Machado, G.; Devine, D.M.; Crespo, J.S.; Giovanela, M. Synthesis and Characterization of Silver Nanoparticles for the Preparation of Chitosan Pellets and Their Application in Industrial Wastewater Disinfection. *Water* **2023**, *15*, 190. [CrossRef]
- 45. Hu, J.; Li, M.; Gao, Q.; Niou, C.; Chien, K. Energy Dispersive Spectrum (EDS) Study of Copper Grid Effect on Semiconductor Failure Analysis. In Proceedings of the ISTFA 2006, ASM, Austin, TX, USA, 12–16 November 2006; Paper No: istfa2006p0297. pp. 297–299. [CrossRef]
- 46. Sharma, V.K.; Yngard, R.A.; Lin, Y. Silver nanoparticles: Green synthesis and their antimicrobial activities. *Adv. Colloid Interface Sci.* **2009**, 145, 83–96. [CrossRef]
- 47. Ahmed, S.; Saifullah; Ahmad, M.; Swami, B.L.; Ikram, S. Green synthesis of silver nanoparticles using *Azadirachta indica* aqueous leaf extract. *J. Radiat. Res. Appl. Sci.* **2016**, *9*, 1–7.

Appl. Nano 2025, 6, 22 15 of 15

48. Rajeshkumar, S.; Malarkodi, C. In vitro antibacterial activity and mechanism of silver nanoparticles against foodborne pathogens. *Bioinorg. Chem. Appl.* **2014**, 2014, 581890. [CrossRef] [PubMed]

- 49. Salazar-Bryam, A.M.; Yoshimura, I.; Santos, L.P.; Moura, C.C.; Santos, C.C.; Silva, V.L.; Lovaglio, R.B.; Costa Marques, R.F.; Jafelicci Junior, M.; Contiero, J. Silver Nanoparticles Stabilized by Ramnolipids: Effect of PH. *Colloids Surf. B Biointerfaces* 2021, 205, 111883. [CrossRef]
- 50. Csapó, E.; Patakfalvi, R.; Hornok, V.; Tóth, L.T.; Sipos, Á.; Szalai, A.; Csete, M.; Dékány, I. Effect of PH on Stability and Plasmonic Properties of Cysteine-Functionalized Silver Nanoparticle Dispersion. *Colloids Surf. B Biointerfaces* **2012**, *98*, 43–49. [CrossRef]

Disclaimer/Publisher's Note: The statements, opinions and data contained in all publications are solely those of the individual author(s) and contributor(s) and not of MDPI and/or the editor(s). MDPI and/or the editor(s) disclaim responsibility for any injury to people or property resulting from any ideas, methods, instructions or products referred to in the content.